ScienSage

Journal of Advanced Scientific Research

Available online through http://www.sciensage.info

ISSN
0976-9595
Research Article

SYNTHESIS AND CHARACTERIZATION OF CARBON BALLS LOADED SILVER ORTHOPHOSPHATE FOR ENVIRONMENTAL REMEDIATION

Inbasekaran Muthuvel[1,2], Baskaran Suwetha[2], Sugumaran Suguna[2], Kaliyamoorthy Gowthami[1], Ganesamoorthy Thirunarayanan[1], Thirugnanam Rajachandrasekar*[2]

[1]*Advanced Photocatalysis Laboratory, Department of Chemistry, Annamalai University, Annamalainagar, Tamilnadu, India*

[2]*Department of Chemistry, M.R. Govt. Arts College, Mannargudi, Tamilnadu, India*

**Corresponding author: proftrchem1966@gmail.com*

ABSTRACT

A silver orthophosphate (Ag_3PO_4) is an efficient photocatalyst. It was successfully synthesized by chemical precipitation method using Ag_3NO_3 and Na_2HPO_4. The resulting Ag_3PO_4 was coated with carbon balls by solid state dispersion method. The products were characterized using X-ray diffraction (XRD), Fourier transform infrared (FT-IR), Scanning electron microscopy- Energy-dispersive X-ray (SEM-EDX) colour mapping and Ultraviolet-Visible diffuse reflectance (UV-DRS). Under UV light, the carbon balls loaded photocatalyst exhibit enhanced photocatalytic activity for the removal of Methyl Violet dye. The effect of operational parameters such as effect of pH, catalyst suspension, initial dye concentration and reusability were observed. Hence, the photocatalyst can be used for multiple runs.

Keywords: Photocatalytic activity; Carbon balls; Ag_3PO_4; Methyl violet, Wastewater treatment.

1. INTRODUCTION

Water is a clear, tasteless, odourless and almost colourless chemical liquid that is the main component of the streams of the earth, the seas of lakes and the fluids of most living organisms. Even though it offers no calories or organic nutrients, it is essential for all known forms of life. For its capacity to dissolve several substances, water is also known as the universal solvent. Unfortunately, since enormous dyes, pesticides, cosmetics, fertilisers, inorganic salt and other chemicals etc. are dissolved to produce polluted water, which has become a major challenge to our existence; this water property contributes to pollution. Therefore, we need to draw urgent attention to purify water. Several techniques have been used to do this, but photocatalysis is commonly used in the wastewater treatment and plays an important role in the remediation of water. Since photocatalysis is a green chemical route, it is therefore essential of the day.

The photocatalysis mechanism is very simple: the UV radiation from sunlight is harnessed by a catalyst and the energy is used to break down various substances. Photocatalysis is used to decompose a broad range of organic materials, organic acids, estrogens, pesticides, dyes, crude oil, microbes (including viruses and chlorine-resistant organisms), inorganic molecules such as nitrous oxides (NOx) and can also eliminate metals (such as mercury) in association with precipitation or filtration [1-3].

As sunlight is used, the technology of solar photo-catalysis is cost efficient and environment friendly approach. The requisite equipment is minimal and suitable even for developing countries or remote locations without electricity access [4-6]. Due to this universal applicability, photocatalysis with nanoparticles as catalysts is used for antibacterial, deodorizing, air purifying, antifogging, self-cleaning and water purify-cation [7-11]. Ag_3PO_4 as a photocatalyst has attracted enormous attention in recent years due to its great potential in harvesting solar energy for environ-mental purification and fuel production.

The photocatalytic performance of Ag_3PO_4 strongly depends on its morphology, dye concentration, duration and amount of radiations irradiating its surface. In addition to high positive aspects of Ag_3PO_4, it still suffers from some major drawbacks. Extremely small size of Ag_3PO_4 based photocatalysts makes their removal from water difficult after use. So, they are immobilized onto various substrates such as activated carbon, clay, polyamide, polyethylene terephthalate, polyacrylonitrile, polyurethane and polyester [12, 13]. Herein, authors have demonstrated the synthesis of

Carbon balls loaded Ag_3PO_4 nanocomposite. Structural analysis of C/Ag_3PO_4 nanocomposite has been carried out using XRD, FT-IR, SEM-EDX colour mapping and UV-DRS. Its photocatalytic efficiency has been tested for the degradation of methyl violet dye. Effect of various parameters such as dye concentration, effect of pH, catalyst suspension and reusability has also been studied for the photodegradation process. Hence, the photocatalyst can be used for multiple runs.

2. EXPERIMENTAL

2.1. Material and Methods

The commercial Methyl violet (MV) (C.I-42535) from Merck Specialities Pvt. Ltd, Silver nitrate (Rankem), Disodium hydrogen phosphate (Qualigens), dextrose, NaOH, H_2SO_4 from (Himedia) were used as received. Ferrous ammonium sulfate, Analar silver sulfate (Himedia), Mercury (II) sulfate (Merck 90%), Potassium dichromate, Ferroin indicator (SD fine) solutions were used as received for Chemical Oxygen Demand analysis. The experimental solution was prepared using distilled water.

2.2. Synthesis of Ag_3PO_4

In a typical synthesis, Na_2HPO_4 aqueous solution (100mL, 0.2M) was added drop wise to the aqueous solution $AgNO_3$ (100mL, 0.6M) and the obtained golden yellow precipitates were collected by filtration, washed with distilled water repeatedly and dried in vacuum at 80°C for 6h.

2.3. Synthesis of Carbon balls

About 5 g of dextrose was dissolved in 50 mL of deionised water. The mixture was then transferred in a 100 mL Teflon-lined stainless-steel autoclave and heated at 180°C for 8 h. After the autoclave was cooled to room temperature, the resulting products were separated by centrifugation washed with absolute ethanol for 4 times and dried in vacuum at 80°C for 12 h.

2.4. Synthesis of Carbon balls loaded Ag_3PO_4 (C/Ag_3PO_4)

About 0.500g of Ag_3PO_4 coated with carbon ball (x wt%; where x = 3, 5, 7, 9%) was prepared by solid state dispersion method using ethanol as solvent. After the coupled semiconductor system was dried at 100°C for 2h. Then it was used as a photocatalyst.

2.5. Photocatalytic degradation experiments

In all experiments, 50 mL of the dye solution containing appropriate quantity of the Carbon loaded Ag_3PO_4 was used. The suspension was stirred for 30 min in dark and then it was irradiated. The solution and dye were continuously aerated by a pump to provide oxygen and for complete mixing of reaction medium. At specific time interval, 2 to 3 mL of the sample was withdrawn and centrifuged to separate the catalyst. One milliliter of the centrifugate was diluted to 10 mL and its absorbance was measured at 580 nm using UV-Visible spectrophotometer to determine the concentration of dye. From the concentration of dye during the degradation process, percentage of dye remaining was determined by the formula:

$$\%\ Degradation = \frac{Ao-A}{Ao} \times 100 \qquad (1)$$

where A_o is the initial methyl violet concentration and A is the final concentration of methyl violet at time t (min).The photocatalytic degradation of MV containing Carbon ball loaded Ag_3PO_4 nanocatalyst obey *pseudo*-first order kinetics. At low initial dye concentration, the rate expression is given by equation (2)

$$d[C]/dt = k'[C] \qquad (2)$$

where k′ is the *pseudo*-first order rate constant. The dye is adsorbed onto the catalyst surface and adsorption-desorption equilibrium is reached in 10 min. After adsorption, the equilibrium concentration of the dye solution is determined, and it is taken as the initial dye concentration for kinetic analysis.

Integration of eqn. (2) (with the limit of $C = C_0$ at $t = 0$ with C_0 being the equilibrium concentration of the bulk solution) gives equation (2).

$$\ln (C_0/C) = k't \qquad (3)$$

where C_0 is the equilibrium concentration of dye and C is the concentration at time t. *pseudo*-First order rate constant k′ was determined from the plot of $\ln C_0/C$ *Vs* t.

2.6. Characterization

The synthesized nanocomposite was characterized using FT-IR, XRD, SEM-EDX, ECM and UV-DRS techniques, the details of which have been provided in a previous work [14, 15]. Chemical oxygen demand (COD) was determined by following the protocol mentioned earlier in the literature [16].

3. RESULTS AND DISCUSSION

3.1. Powder XRD analysis

X-Ray Diffraction (Fig.1) shows that the standard XRD pattern of the Ag_3PO_4 (Fig.1a) and prepared C/Ag_3PO_4 (Fig. 1b). All diffraction peaks in XRD patterns of Ag_3PO_4 and C/Ag_3PO_4 can be indexed to the body-centered cubic structure of Ag_3PO_4 (JCPDS No. 06-0505). The characteristic peaks of Ag_3PO_4 at 2θ

values 21.10, 29.99, 32.98, 38.61, 43.02, 48.10 53.39, 55.10, 57.55, 62.5, 70.01, 73.11 and 75.02 correspond to (110), (200), (210), (211), (220), (310), (222), (320), (321), (400), (420), (421) and (332) are well matched with the earlier report [17].

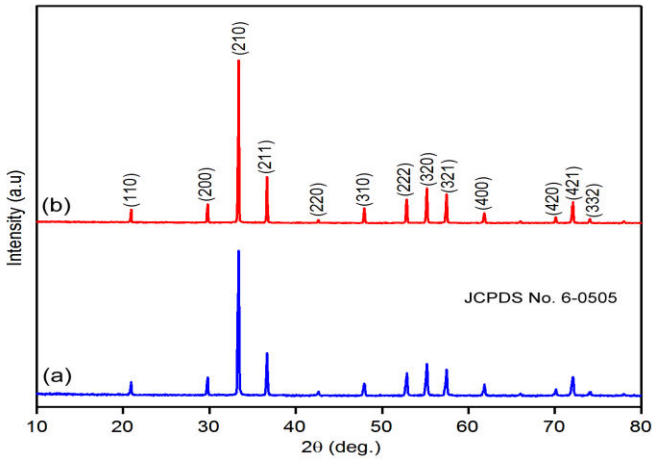

Fig. 1: XRD patterns of a) Ag_3PO_4 and b) C/Ag_3PO_4

3.2. FT-IR spectrum

FT-IR of prepared Ag_3PO_4 sample and C/ Ag_3PO_4 are shown in Fig. 2. The two peaks at 3420 and 1650 cm^{-1} are related to the -OH stretching and bending vibrations of adsorbed H_2O molecules. The peak at around 540 cm^{-1} is ascribed to the O=P-O bending vibration, while the peaks at 850 and 1097 cm^{-1} are due to the symmetric and asymmetric stretching vibrations of P-O-P rings. One strong band featured at 1383 cm^{-1} derives from the stretching vibration of doubly bonded oxygen (P=O) and the harmonics of the above modes [18]. After Carbon balls loaded to Ag_3PO_4 there is no significant change in vibration stretching modes in this spectrum.

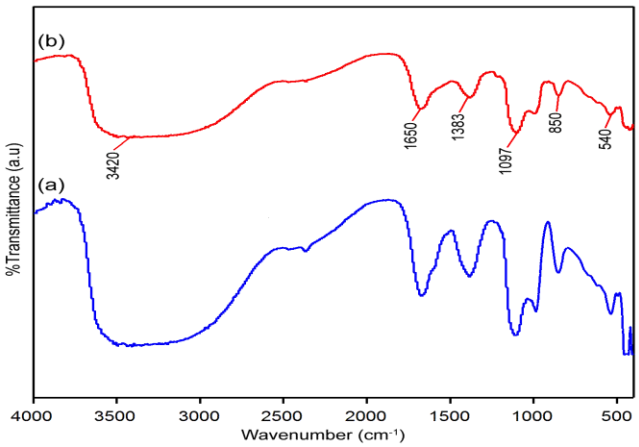

Fig. 2: FT-IR spectra of a) Ag_3PO_4 and b) C/Ag_3PO_4

3.3. SEM-EDX color mapping

SEM images of prepared C/Ag_3PO_4 are shown with different magnifications reveal that the particles are not well shaped (Fig. 3a-d). In Fig. 3a and b shows fully agglomerated with different micrometer magnifications. Carbon spheres are clearly shown in Fig. 3c and d. The presence of the elements Ag, P, O and C in the catalyst are confirmed by EDX analysis from the particular selected area (Fig. 4). The EDX analysis revealed that the relative atoms are present in the prepared sample. To confirm the presence of these elements C/Ag_3PO_4 was analyzed by elemental mapping (Fig. 5). The different color areas in Fig. 5 indicate Ag, P, C and O enriched areas of the sample.

3.4. UV-DRS analysis

The optical properties of C/Ag_3PO_4were explored by UV-Vis diffuse reflectance spectroscopy. The DRS of Ag_3PO_4 and C/Ag_3PO_4 catalysts are displayed in fig. 6. C/Ag_3PO_4 (fig.6b) shows an increased absorption over the Ag_3PO_4 (fig.6a) material in the visible regions. This reveals that C/Ag_3PO_4can be used as a visible light active semiconductor photocatalyst material. Kubelka -Munk plots for Ag_3PO_4 and C/Ag_3PO_4 are shown in Fig. 7. The optical band gap of Ag_3PO_4 (fig.7 a) and C/Ag_3PO_4 (Fig. 7 (b) is calculated to be 2.44 and 2.41 eV, respectively.

3.5. Photocatalytic Activity Of Carbon Balls Loaded Ag_3po_4nanocomposite (C/Ag_3po_4)

3.5.1. Primary Analysis

The photocatalytic activity of the C/Ag_3PO_4 nanocomposite was analyzed by the degradation of MV. Controlled experiments under different conditions were carried out and the results are displayed in Fig. 9. In the presence of dye/ Ag_3PO_4 /dark a decrease (14%) in dye concentration occurs and remains almost constant up to 90 min (curve a). The dye on irradiation with Ag_3PO_4 under UV light undergoes 95% degradation in 25 min (curve b). The dye on irradiation with different carbon wt% loaded Ag_3PO_4under UV light shows (curves c, d, e & f). 5wt% C/Ag_3PO_4shows maximum degradation (99%, 25mins) efficiency compared to others. A decrease (25%) in dye concentration was observed when dye is treated with 5wt% C/ Ag_3PO_4 in dark (curve g).

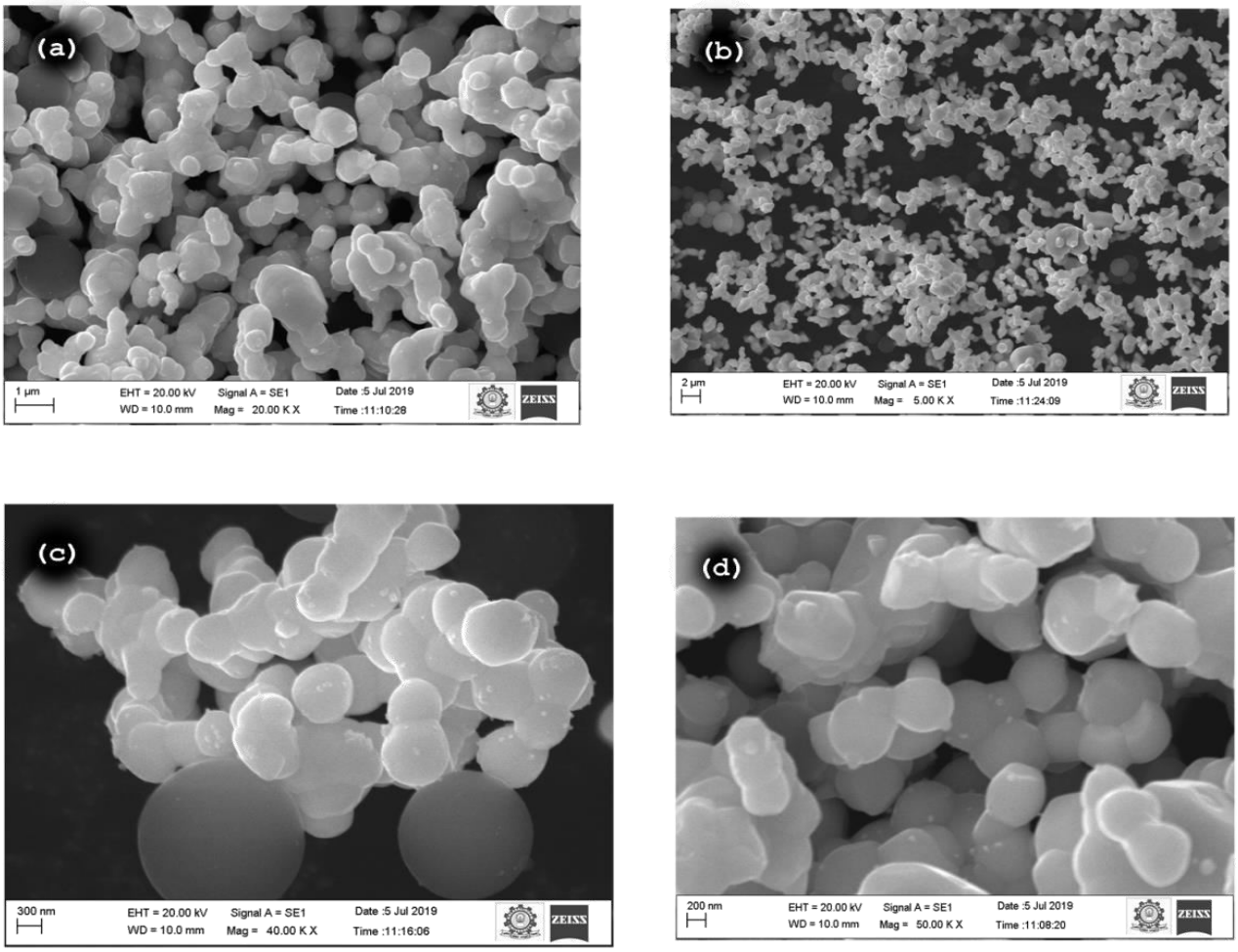

Fig. 3: SEM images of C/Ag_3PO_4

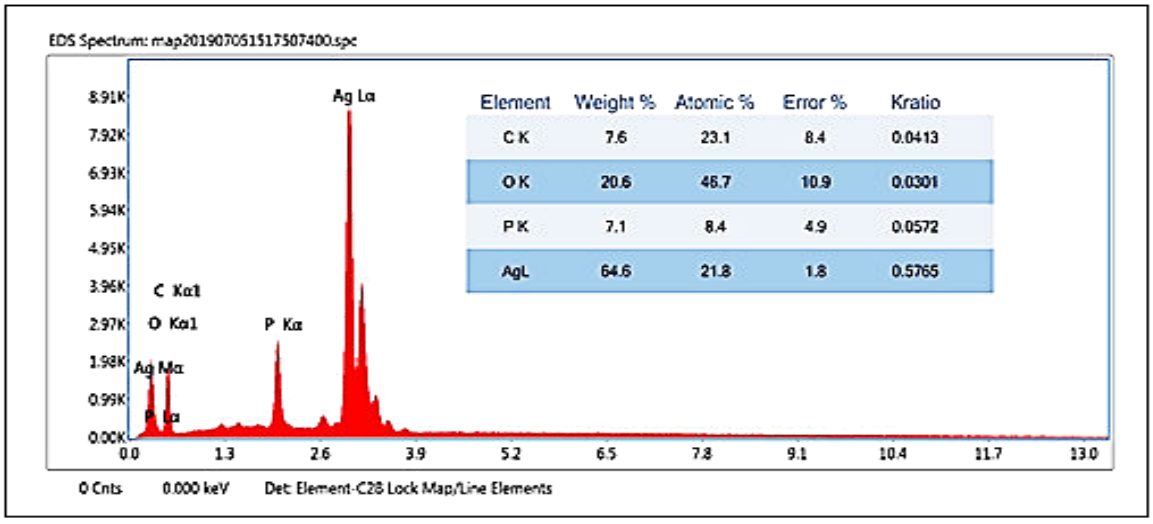

Fig. 4: EDX image of C/Ag_3PO_4

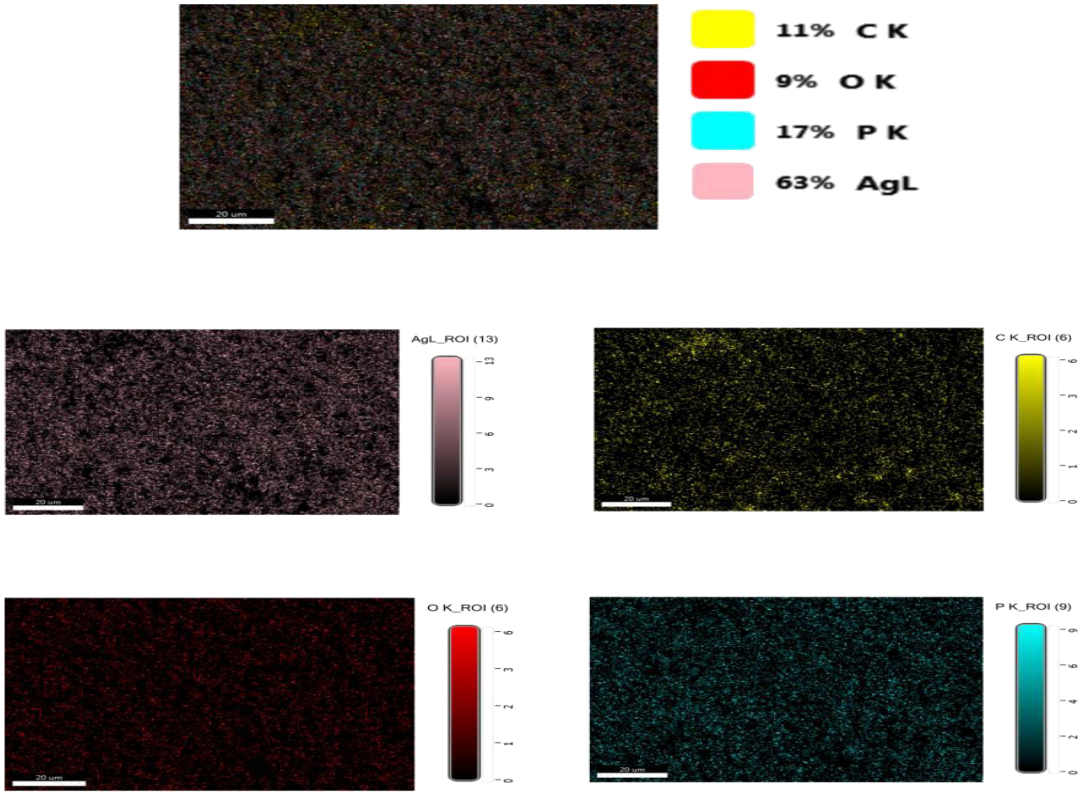

Fig. 5: Colour mapping images of C/Ag_3PO_4

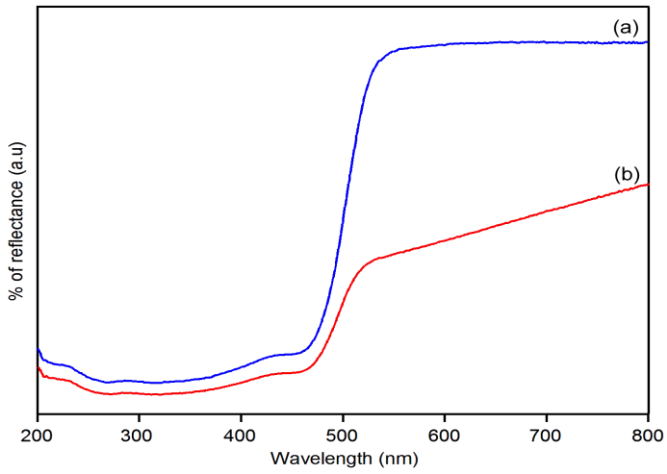

Fig. 6: DRS of a) Ag_3PO_4 and b) C/Ag_3PO_4

3.5.2. *Effect of catalyst loading*

The study on degradation rate with different amounts of catalyst is important to find out the minimum amount of catalyst required for maximum dye removal. Hence, it is required to optimize the dose of catalyst for the effective mineralization of MV. The experiment was carried out by varying catalyst concentration from 0.6 to 1.4 g L^{-1} in aqueous MV solution under UV-A light irradiation for 20 min. The increase of catalyst weight from 0.6 to 1.4 g L^{-1} increases the degradation from 74 to 90% at the time of 10 min (Fig. 9). Further increase of catalyst amount (above 1.4 g L^{-1}) sudden decreases the rate constant. The decrease in efficiency of MV at higher amount (above 1.4 g L^{-1}) caused by result in the agglomeration of catalyst resulting in the unavailability of the surface for photon harvesting [19]. The optimum amount of catalyst for efficient degradation of MV is 1.4 g L^{-1}.

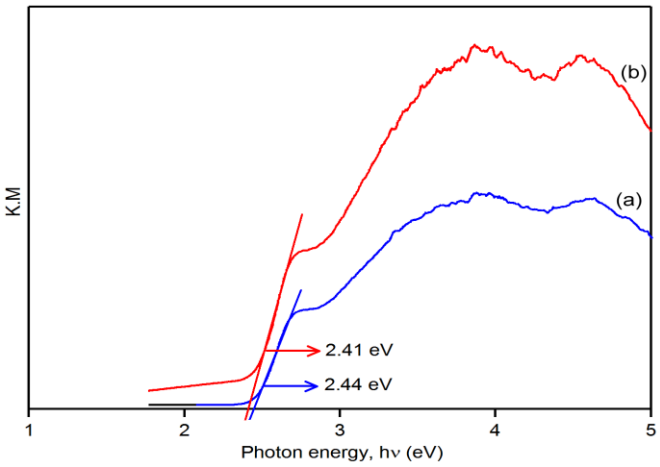

Fig. 7: K.M plot of a) Ag_3PO_4 and b) C/Ag_3PO_4

3.5.3. *Influence of initial solution pH*

The pH of solution plays a vital role in photocatalytic degradation. The effect of pH ranges from 3-9 was studied, and the results are shown in Fig. 10. At pH 7, the maximum percentage of 99% degradation was observed (25 min). Above pH 7, the degradation efficiency decreases. At low pH, the removal efficiency is less due to the dissolution of C/Ag_3PO_4. Degradation efficiency of a catalyst depends on the adsorption of dye molecules. The percentages of adsorption at pH 3, 5, 7 and 9 were found to be 9.7, 19.3, 19, 21.5 and 15.3 at equilibrium, respectively. Since the adsorption is maximum at pH 7, the degradation is high at this pH. At pH above 7, surface of catalyst is negatively charged and the electrostatic attraction between dye anion and negatively charged catalyst becomes weak resulting in decreased adsorption [20, 21]. This decreases the degradation at above pH 7. Hence, pH 7 is the optimum pH for the mineralization of MV.

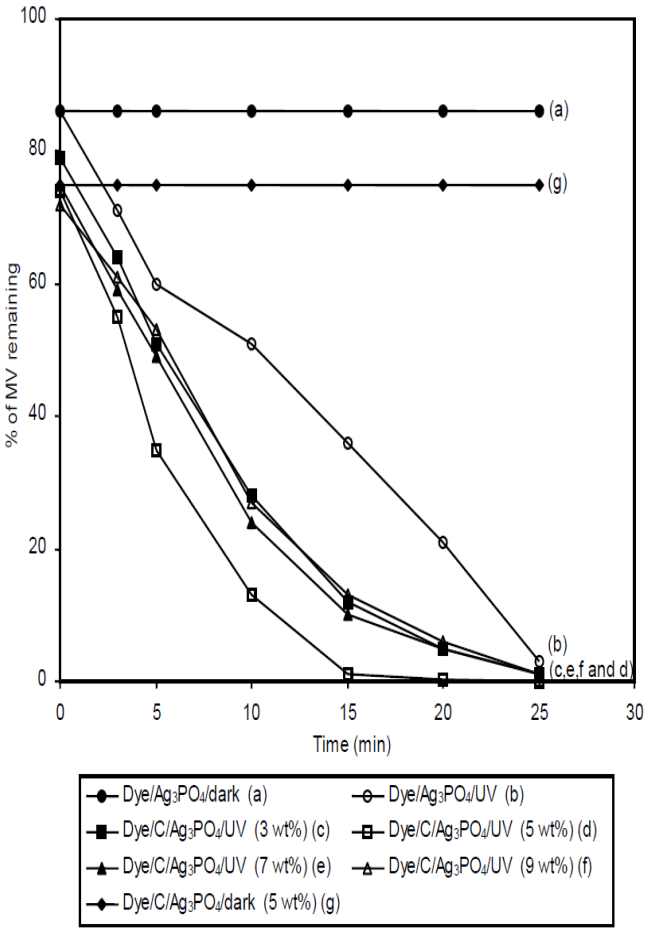

Fig. 8: Primary analysis [MV] = 3×10^{-4} M, catalyst suspended=1.0 g L^{-1}, airflow rate=8.1 mL s^{-1}, pH = 7

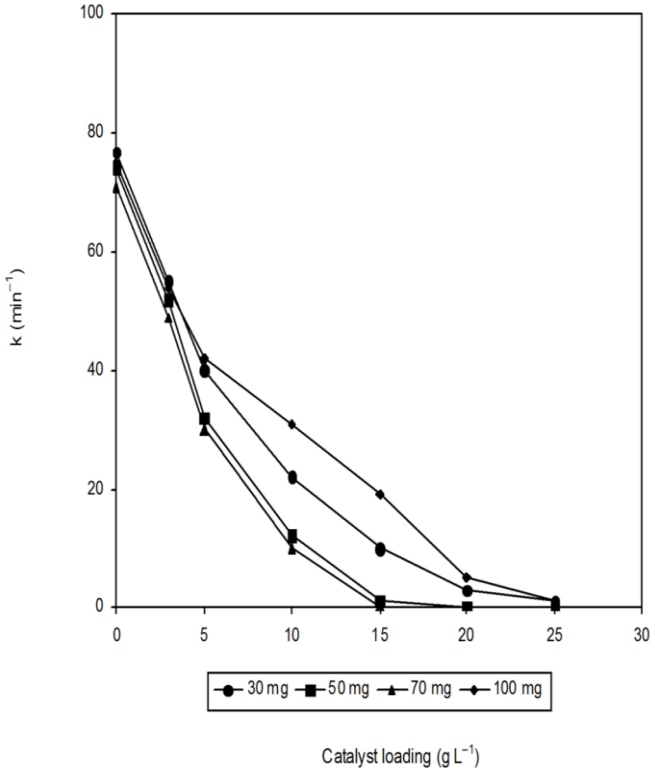

Fig. 9: Effect of catalyst loading. [MV] = 3×10^{-4} M, airflow rate = 8.1 mLs^{-1}, pH = 7, irradiation time= 25 min

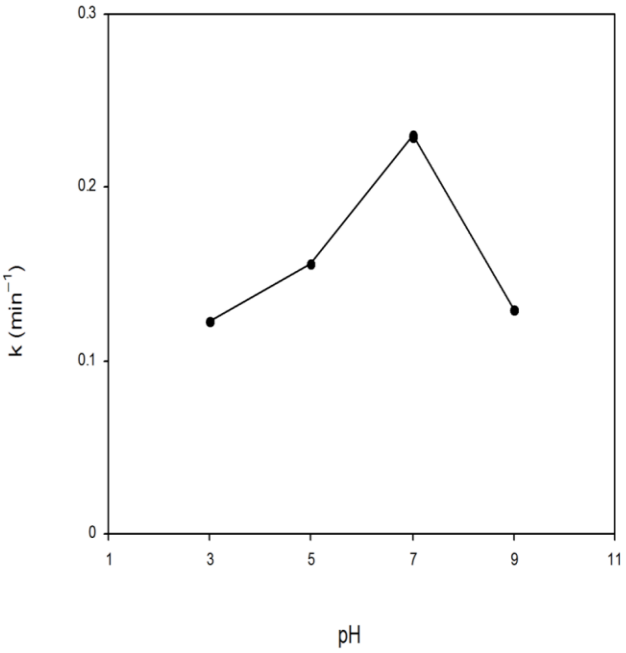

Fig. 10: Effect of initial solution pH. [MV]= 3×10^{-4} M, catalyst suspended = 1.4 g L^{-1}, airflow rate = 8.1 mL s^{-1}, irradiation time =10 min.

3.5.4. Effect of initial dye concentration

As the dye concentration is an important parameter in wastewater treatment, the effect of initial dye concentration of MV on the degradation was investigated over the concentration of 1 to 5 × 10^{-4} M. Increase the initial dye concentration from 1 to 5 × 10^{-4} M decreases the degradation rate constant from 0.461 to 0.034 min^{-1} (Fig. 11) at the time of 20 min. The catalyst amount and UV power remains in all experiments same. The generation of hydroxyl radical remains constant. The rate of degradation is related to the $OH^{\bullet}$ radical formation on catalyst surface and probability of $OH^{\bullet}$ radical reacting with dye molecule. When the initial concentration of the dye increases, the path length of photon entering into the solution decreases and the photocatalytic degradation efficiency also decreases [22, 23].

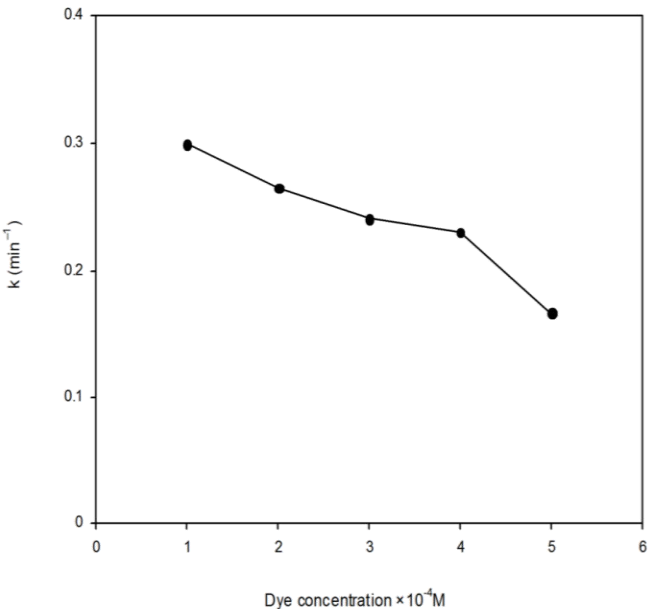

Fig. 11: Effect of initial dye concentration. Catalyst suspended = 1.4 g L^{-1}, airflow rate = 8.1 mL s^{-1}, pH = 7, irradiation time = 20 min.

3.5.5. Long-term stability

The recyclability results of catalyst are shown in fig. 12. To test reusability of C/Ag_3PO_4 under identical reaction conditions, the catalyst was recovered and used for further cycles. The results of C/Ag_3PO_4 exhibit excellent photostability and almost 97% degradation was observed for all the five cycles. There is no significant change in the degradation efficiency of C/Ag_3PO_4 after 5th cycle. This makes the catalyst suitable for continuous treatment of wastewater.

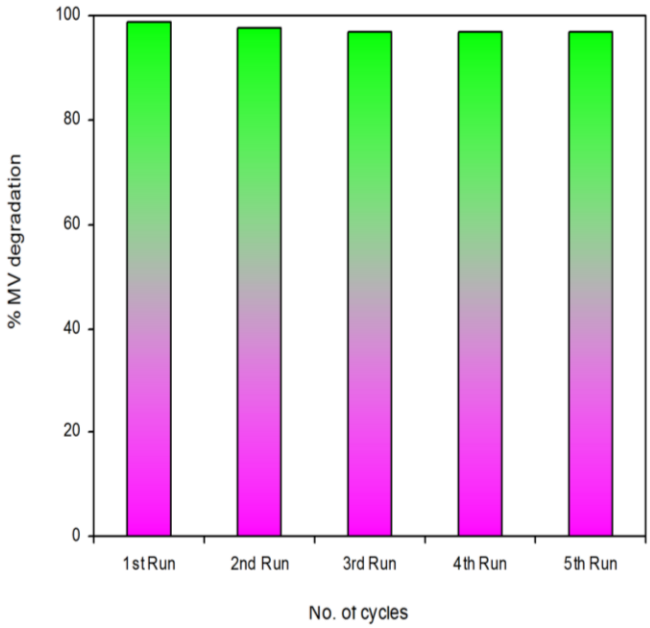

Fig. 12: Long-term stability. [MV] = 3×10^{-4} M, catalyst suspended = 1.4 g L^{-1}, airflow rate = 8.1 mL s^{-1}, pH = 7, irradiation time = 25 min

3.6. Carbon Balls Loaded Ag_3po_4photocatalytic Mechanism

The enhancement of higher efficiency of the 5% wt C/Ag_3PO_4 for the degradation of methyl violet (MV) presumably results due to the adsorption of dye on Carbon spheres effectively on during adsorption experiment. Under UV light irradiation, the C/Ag_3PO_4 nanocatalyst were excited to form electrons (e^-) in conduction band and holes (h^+) in valence band. Subsequently, the photoexcited electrons in conduction band of C/Ag_3PO_4 was transferred to the adsorbed O_2 on the surface of C/Ag_3PO_4 to form $O_2^{\bullet-}$ radicals. Concurrently, OH^-/H_2O ions/molecules were protonated by H^+ on valence band of Ag_3PO_4 to form $^{\bullet}OH$ radicals. Finally, $O_2^{\bullet-}$ and $^{\bullet}OH$ radicals attacked the MV molecules to form decomposed molecules, such as CO_2 and water.

3.6.1. COD Measurements

In order to confirm the mineralization of dye, COD measurements were made for the degradation of MV with C/Ag_3PO_4under optimum conditions. COD reduction values for the dye at different times of UV irradiation are given in Table 1. COD values show 95% COD reduction (MV) for 60 min UV irradiation. These results confirm the mineralization of the dye with C/Ag_3PO_4 process.

Table 1: COD measurements under optimum conditions

Catalyst	0 min	10min	20 min	30min	60 min
	COD reduction (%)				
C/Ag_3PO_4	0	40	61	87	95

[MV] = 3×10^{-4} M, catalyst suspended = 1.4 g L^{-1}, airflow rate = 8.1 mL s^{-1}, pH = 7, irradiation time = 120 min

4. CONCLUSIONS

Silver orthophosphate was successfully synthesized by chemical precipitation method and it was coated with carbon balls by solid state dispersion method. XRD patterns of Ag_3PO_4 and C/Ag_3PO_4 can be indexed to the body-centered cubic structure of Ag_3PO_4 (JCPDS No. 06-0505). FTIR spectrum reveals that presence of the peak at 540 cm^{-1} due to the O=P-O bending vibration, while the peaks at 850 and 1097 cm^{-1} are due to the symmetric and asymmetric stretching vibrations of P-O-P rings. SEM images of prepared C/Ag_3PO_4 are shown with different magnifications reveal that the particles are not well shaped shows fully agglomerated with different micrometer magnifications. Carbon spheres are clearly shown and the presence of the elements Ag, P, O and C in the catalyst are confirmed by EDX and ECM analysis. The DRS of C/Ag_3PO_4 shows an increased absorption than the Ag_3PO_4 in the visible regions. This reveals that C/Ag_3PO_4 can be used as a visible light active semiconductor. Under UV light the carbon balls loaded photocatalyst exhibit enhanced photocatalytic activity for the removal of Methyl Violet dye. The effect of operational parameters reveals that the optimum pH and catalyst suspension are 7 and 1.4gL^{-1} for complete degradation of the MV. The photocatalyst can be used for multiple runs all the runs gave almost 97% degradation was observed. COD reduction (95%) confirms that the mineralization of the dye with C/Ag_3PO_4 process. Hence it is industrial feasible, applicable and economical material for wastewater treatment.

5. ACKNOWLEDGMENT

One of the authors (I. Muthuvel) thanks financial support from the University Grants Commission (UGC), New Delhi, for through research grant No. UGC sanctioned letterF.No-43-222/2014(SR).

6. REFERENCES

1. Kwon S, Fan M, Cooper A. *Crit. Rev. Environ. Sci. Tech*,2008; **38:**197-226
2. Yao Y, Yang Z, Sun H, Wang S. *Ind. Eng. Chem. Res,* 2012; **51:**14958-14965
3. Yao Y, Xu C, Qin J, Wei F, Rao, M. *Ind. Eng. Chem. Res,* 2013; 52**:**17341-.17350
4. Wang M, Han J, Hu Y, Guo R. *RSC Adv,* 2017; **7:** 15513-15520.
5. Wang X J, Yang WY, Li FT, Xue YBR, Liu H, Hao YJ. *Ind. Eng. Chem. Res,*2013; **52 :**17140-.17150.
6. Katsumata H, Sakai T, Suzuki T, Kaneco S. *Ind. Eng. Chem. Res*, 2014; **53:**8018-8025.
7. Gowthami K, Arumugam M, Dinesh Kumar N, Thirunarayanan G, Krishnakumar B, Swaminathan M, Muthuvel I. *J Adv. Sci. Res,* 2020; **11:**116-119.
8. Muthuvel I, Gowthami K, Thirunarayanan G, Krishnakumar B, Swaminathan M, Siranjeevi R. *Environ. sci. Pollut. Res,* 2020; **27:**43262-43273.
9. Dong F, Ou M, Jiang Y, Guo S, Wu Z. *Ind. Eng. Chem. Res,* 2014; **53:** 2318-2330.
10. Gowthami K, Krishnakumar B, Thirunarayanan G, Swaminathan M, Muthuvel I. *Materials Today: Proceedings,* 2020; **29:**1199-1203.
11. Srishankar J, Muthuvel I, Sobana N. *Inorg. Chem. Commu.,* 2021; **123:**108306.
12. Walker GM, Weatherley LR. *Water Res*, 1997; **31:** 2093-2101.
13. Yang M Q, XuY J. *J. Phys. Chem,* 2013; **117C:**21724-21734.
14. Suppuraj P, Thirumalai K, Parthiban S, Swaminathan M, Muthuvel I. *J. Nanosci. Nanotechnol*, 2019; **19:**1-10.
15. Gowthami K, Krishnakumar B, Sobral AFJN, Thirunarayanan G, Swaminathan M, Siranjeevi R, Rajachandrasekar R, Muthuvel I. *J. Cluster Sci,* 2020; **31:**839-849.
16. Muthuvel I, Krishnakumar B, Swaminathan M. *Indian J. Chem,* 2014; **53A:**672-678.
17. Chen Z, Wang W, Zhang Z, Fang X. *J. Phys. Chem,* 2013; **117C:**19346-19352.
18. Choi J, Sudhagar P, Kim JH, Kwon J, Kim J, Terashima C, et al. *Phys. Chem. Chem. Phys*, 2017; **19:**4648-4655.
19. Muneeb M, Ismail B, Fazal T, Ali Khan R, Muhammad Khan A, Bilal M, et al. *Arabian J. Chem,* 2018; **11:**1117-1125.

20. Hussien MSA, Yahia IS. *J. Photochem. Phtobiol A Chem*, 2019; **368:** 210-218.
21. Rajasri S, Krishnakumar B, Sobral AFJN, Bala chandran S, Swaminathan M, Muthuvel I. *Mater. Today Proc*, 2019; **15:** 471-480.
22. Khataee A, Kalderis D, Gholami P, Fazli A, Moschogiannaki M, Binas V, et al. *Appl. Surface Sci,* 2019; **498:** 143846.
23. Muthuvel I, Gowthami K, Thirunarayanan G, Suppuraj P, Krishnakumar B, Sobral AFJN, Swaminathan M. *Int. J. Ind. Chem,* 2019; **10:**77-87.